URSI GASS 2021, Rome, Italy, 28 August - 4 September 2021

Modeling and Realization of a 24-GHz FMCW Radar for Accurate Target Distance Identification

Stefano Pisa, Gabriel Adrian Mihu, and Emanuele Piuzzi

Department of Information Engineering, Electronics and Telecommunication, Sapienza University of Rome, Rome, Italy

Abstract

In this work, the modeling and realization of a 24-GHz Radar based on the BGT24MTR11 chipset is presented. The model has been implemented with the Visual System Simulator (VSS) tool available inside the AWR software. Two modular implementations of the designed Radar have been proposed. One in which the Radar is driven by a DAQ card from National Instruments and one in which the Radar is controlled by a PLL circuit. The circuit model has been validated through a comparison with analytical and experimental measurements considering as target a metallic sphere. The better performance of the architecture with the PLL has been also evidenced by considering a scenario with a panel target.

1 Introduction

In recent years, Radar systems have been widely used in various fields such as defense, automotive, navigation, traffic control and environmental monitoring, but also in fields such as medicine and sport [1]. One of the main advantages of Radars is their ability to work in unfavorable environmental conditions. Other advantages of Radar systems compared to technologies such as lasers and ultrasounds, are the possibility of identifying radial movements of the targets, their relative insensitivity to the environment (rain, snow, dust, etc.) and the ability to penetrate non-metallic materials.

Various type of Radars were proposed in literature like Doppler [2]-[3], ultrawideband [4]-[5], and Frequency Modulated Continuous Wave (FMCW) [6]-[7]. In this paper FMCW Radars have been considered due to some advantages they offer. In particular, the modulation is easily obtainable with commercially available voltage controlled oscillators at medium / low cost, the transmitted signals do not interfere with other radiating systems that are nearby, the data analysis can be performed by a single low cost processor. On the market there are various types of FMCW transceivers that operate in the 24-GHz industrial, scientific, and medical (ISM) band.

Distance2Go is a 24-GHz Radar based on the BGT24MTR11 transceiver chipset from Infineon. The board can measure distance, speed and direction of movement. These features make the board suitable for various applications such as motion detection, presence sensing, proximity sensing, etc. [8].

The EV-TINYRAD24G from Analog-Devices is a Radar evaluation module that allows the implementation and testing of Radar sensing applications. The EV-TINYRAD24G has an integrated antenna array in a multiple input multiple output (MIMO) Radar scheme. The combined antennas allow the TinyRad module to detect the distance, speed, and angular position of multiple targets simultaneously [9]. In order to develop applications based on the various transceivers on the market it is essential to have an accurate model of the chipset and to be able to generate stable and repeatable chirps. In this work, a model of a Radar system was developed using the Visual System Simulator (VSS) tool available inside the AWR software. The model results were compared with analytical solutions and with results of two modular realizations. In the first, the Radar VCO is driven with a National Instruments DAQ board while the second uses a PLL module to generate a frequency stable FMCW signal.

2 Analytical and VSS model of the Radar

An FMCW Radar in its simplest form is shown Fig. 1:

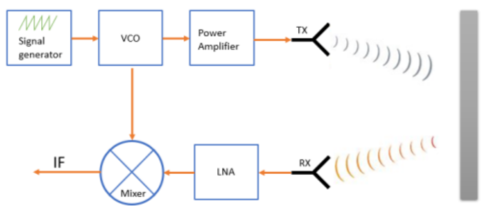

Figure 1. FMCW Radar operation diagram.

In order to compare the results of an analytical model with those of the VSS software and with those of an experimental Radar prototype, the RMS voltage at the mixer output (V_{IF}) was considered. From an analytical point of view, this voltage is given by:

$$V_{IF} = \sqrt{\frac{P_t G_t G_r \sigma \lambda^2 G_{CONV} Z_O}{L_S (4\pi)^3 R^4}} \tag{1}$$

where P_t is the transmitted power, G_t is the gain of the transmitting antenna, G_r is the gain of the receiving antenna, σ is the Radar cross section of the target, λ is the wavelength associated with the propagating signal, G_{CONV} is the conversion gain of the mixer, L_S are the system losses, Z_O is the impedance seen at the mixer output and R is the target distance.

Visual System Simulator is a design and simulation tool for communication and Radar systems. The tool is available within the AWR software and consists of a series of components and libraries useful for simulation at the system level. The simulation diagram shown in Fig. 2 reproduces the block diagram of Fig. 1. The channel-scatterer model is reported in Fig. 3. Basically, the channel introduces a delay due to the propagation time of the electromagnetic wave, attenuates the transmitted signal, models the backscattering with the RCS and introduces Gaussian noise.

3 Modular implementation

The modeled Radar was then built using modules available on the market. The DAQ board controlled SISO Radar is shown in Fig. 4. The Infineon's evaluation board mounts the BGT24MRT11 transceiver [10]. The input and output ports of the board are connected to two PASTERNACK PE9852 / 2F-15 horn antennas. The antennas operate in the 18-26.5 GHz band with a gain of 15 dBi. The DAQ card (NI USB-6361) is controlled by a computer through a LabVIEW program, which generates the sawtooth waveform with a period equal to T=1 ms necessary to drive the VCO and acquires the IF signal coming from the mixer with a sampling frequency of 200 kHz. The PLL driven SISO Radar is shown in Fig. 5. In this case, the Radar VCO is controlled by the evaluation board of the ADF4159 chip [11]. A quartz, mounted on the board, is used to generate the 100 MHz reference frequency. The card can be programmed through a software that Analog Devices makes available, called ADF4158 / 9 [12].

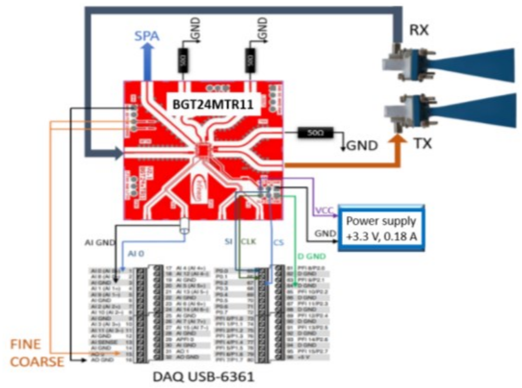

Figure 4. DAQ driven SISO Radar.

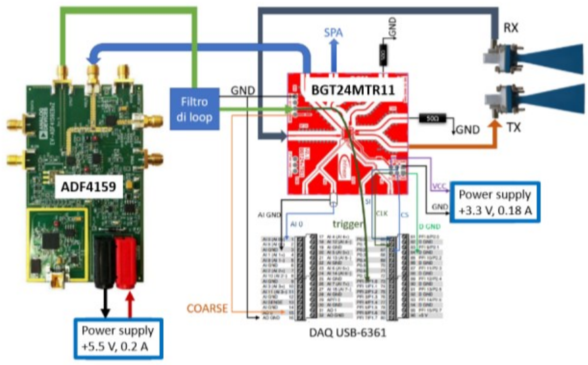

Figure 5. PLL driven SISO Radar.

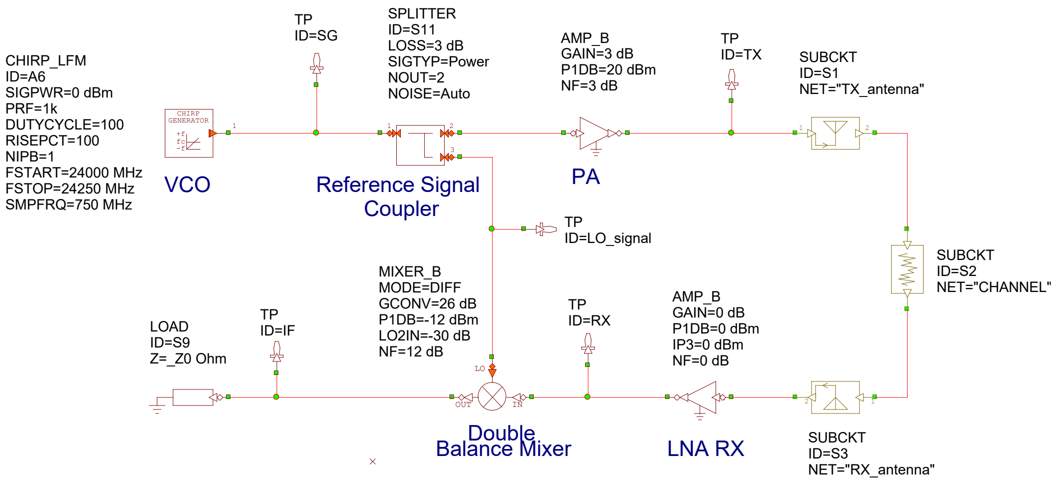

Figure 2. VSS simulation scheme.

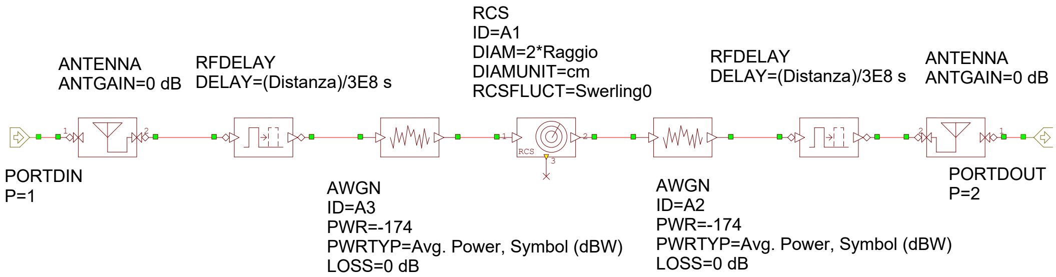

Figure 3. Model of the channel and of the scatterer.

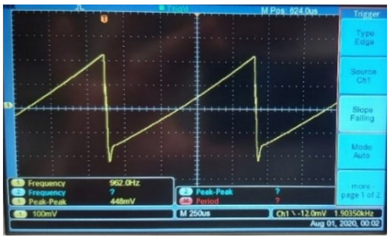

Figure 6. Ramp driving the VCO.

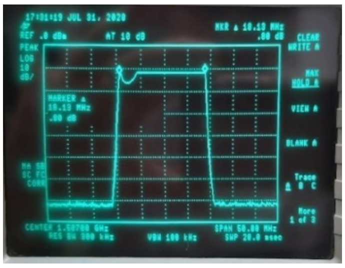

Figure 7. Spectrum of the transmitted signal.

Furthermore, through Analog Devices ADSim PLL software it is possible to simulate the phase-locked loop and size the loop filter [13]. As in the previous case, the DAQ card is used for the IF signal acquisition. To verify the actual operation of the PLL, the ramp driving the VCO was measured with an oscilloscope (see Fig. 6). The spectrum of the transmitted signal, frequency scaled by a factor of 16, is shown in Fig. 7. Note that the spike in Fig. 6 is the responsible of the slight dip of the spectrum in Fig. 7. However, the rising and falling edges of the spectrum are extremely steep indicating the low phase noise produced by the PLL. From Fig. 7 a bandwidth B = 250 MHz was measured.

4 Results

In order to compare the performances of the two experimental boards, measurements were then conducted on a metal panel placed at 1.5 m from the target. Fig. 8 shows the time trend (a) and the spectra (b) of the IF signal obtained when the Radar is driven by the DAQ board. The spectra in Fig. 8 (b) were evaluated by performing the Fast Fourier transform on 200 samples acquired over time (blue curve) or by performing a zero padding of a factor of 2 (red curve) or 10 (green curve). On the other hand, Fig. 9 shows the time trend (a) and the spectra (b) obtained when the Radar is controlled by the PLL board. As shown, the time trend is more regular and the lateral lobes of the spectrum are lower for the data acquired with the Radar with the PLL with respect to the one acquired with the DAQ driven Radar. Since the target distance is given by: $R = f_{peak}\, c\, T/2B$, the peak of the frequency response (f_{peak}) can be converted into the target distance. From Fig. 9(b) it results that the error on the target position is 41 cm, 16 cm, and 7 cm for zero padding equal to 0, 2 and 10, respectively. Therefore, with the use of zero padding it is possible to significantly reduce the measurement error on the target distance.

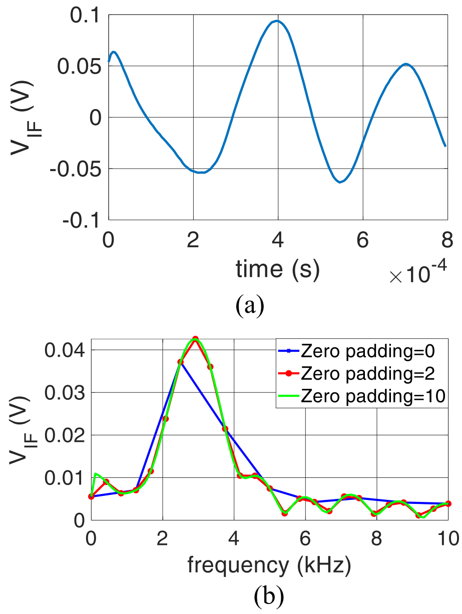

Figure 8. Time course (a) and spectrum (b) of the Radar output signal with DAQ.

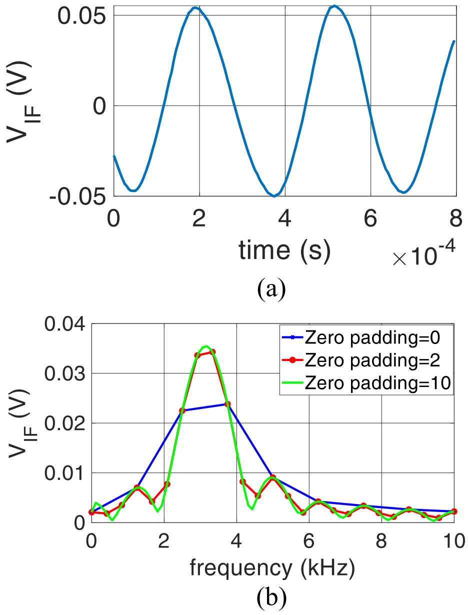

Figure 9. Time course (a) and spectrum (b) of the Radar output signal with PLL.

Then simulations with the VSS Radar model have been compared with analytical results and experimental measurements. The considered scenario consists of a metal sphere with a radius of 15 cm (RCS = 0.07 m^2 or -11.51 dBsm) placed at a distance of 1 m from the Radar antennas. The Radar transmits a power of 0 dBm. Using the VSS model shown in Fig. 2 and Fig. 3, the power levels at the output of the Radar subcomponents are evaluated and reported in Fig. 10. The power of -29.2 dBm at the output of the mixer corresponds to an output RMS voltage over 50 Ω of 7.8 mV. Using (1) V_{IF} = 7.9 mV is achieved, very close to the simulated value. The same scenario was studied experimentally by using the Radar driven by the PLL (see Fig. 11).

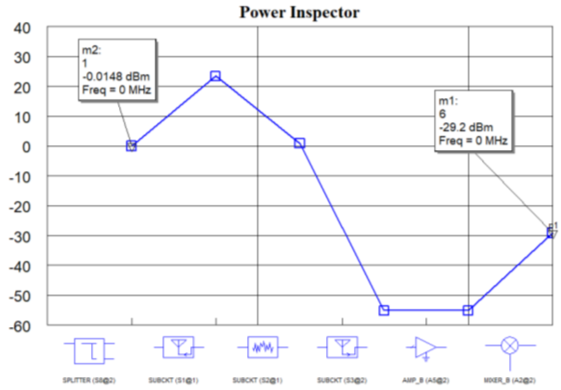

Figure 10. VSS simulated Radar output signal spectrum.

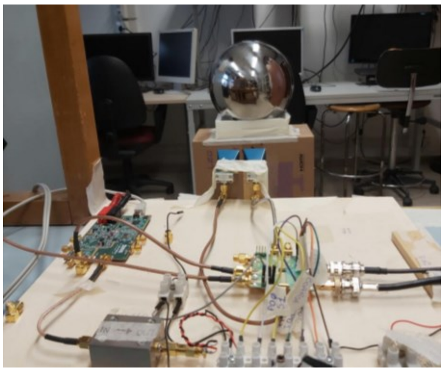

Figure 11. Picture of the considered scenario.

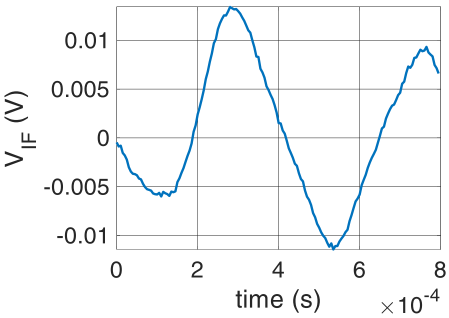

(a)

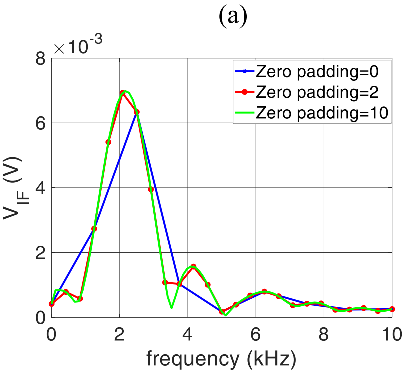

(b)

Figure 12. Time course (a) and spectra (b) of the Radar output signal with PLL for a sphere 1 m far from the Radar antennas.

Fig. 12 shows the time behavior (a) and the spectra (b) of the IF signal. A value of about 7 mV, very close to the simulated one has been obtained.

5 Conclusions

In this work a comparison between a PLL driven and DAQ driven Radar system based on the BGT24MTR11 chipset has been performed. The better performances of the first configuration have been evidenced. Moreover, a system model based on VSS has been realised and validated through analytical and experimental tests. In the future the model will be used to study more complex systems such as MIMO radars used to acquire images of the scenario in front of the Radar.

6 References

1. S. Pisa, E. Pittella, and E. Piuzzi, “A survey of radar systems for medical applications,” *IEEE Aerospace and Electronic System Magazine*, **31**, 11, Part 2, pp. 64-81, November 2016.
2. S. Kim, and C. Nguyen, “On the development of a multifunction millimeter-wave sensor for displacement sensing and low-velocity measurements.“ *IEEE Transactions on Microwave Theory and Techniques*, **52**, 11, pp. 2503–2512, 2004.
3. C. Li, J. Cummings, J. Lam, E. Graves, and W. Wu, “Radar remote monitoring of vital signs,” *IEEE Microwave Magazine*, **49**, pp. 47-56, 2009.
4. McEwan, T. E. Ultra wideband radar motion sensor. United States Patent 5,361,070, 1994.
5. S. Pisa, P. Bernardi, M. Cavagnaro, E. Pittella, and E. Piuzzi, “A circuit model of an ultra wideband impulse radar system for breath-activity monitoring,” *Int. J. Numer. Model.*, **25**, 1, pp. 46-63, 2012.
6. G. Wang, C. Gu, T. Inoue, and C. Li, “A hybrid FMCW-interferometry radar for indoor precise positioning and versatile life activity monitoring, “*IEEE Transactions on Microwave Theory and Techniques*, **62**, 11, pp 2812–2822, 2014.
7. G. Sacco, E. Piuzzi, E. Pittella, S. Pisa, “An FMCW Radar for localization and vital signs measurement for different chest orientations,” *Sensors*, **20**, 12, pp. 1-14, 2020.
8. Infineon Technologies AG. AN543: Distance2Go AppNote BGT24MTR11, 2019
9. Analog Devices UG-1709: Evaluating the TinyRad 24 GHz Demonstration Platform, 2020
10. Infineon Technologies, Data sheet BGT24MTR11: Silicon Germanium 24 GHz Transceiver MMIC, 2014.
11. Analog Devices, Data Sheet ADF4159: Direct Modulation/Fast Waveform Generating, 13 GHz Fractional-N Frequency Synthesizer, 2014.
12. Analog Devices, ADF4158/9/69 PLL software, 2016
13. Analog Devices, ADIsimPLL 5.10, 2019